J. exp. Biol. **116**, 1–25 (1985)
Printed in Great Britain © *The Company of Biologists Limited 1985*

NEUROMUSCULAR TRANSMISSION IN THE JELLYFISH *AGLANTHA DIGITALE*

BY P. A. H. KERFOOT, G. O. MACKIE, R. W. MEECH, ALAN ROBERTS AND C. L. SINGLA

Department of Biology, University of Victoria, British Columbia, Canada V8W 2Y2, Department of Physiology, Medical School, University Walk, Bristol BS8 1TD, U.K. and *Department of Zoology, University of Bristol, Bristol BS8 1UG, U.K.*

Received 5 November 1984

SUMMARY

1. In the jellyfish *Aglantha digitale* escape swimming is mediated by the nearly synchronous activity of eight giant motor axons which make direct synaptic contact with contractile myoepithelial cells on the under-surface of the body wall. The delay in transmission at these synapses was $0{\cdot}7 \pm 0{\cdot}1$ ms ($\pm$S.D.; $N = 6$) at 12 °C as measured from intracellular records. Transmission depended on the presence of Ca^{2+} in the bathing medium. It was not blocked by increasing the level of Mg^{2+} to 127 mmol l^{-1}.

2. The myoepithelium is a thin sheet of electrically coupled cells and injection of current at one point was found to depolarize the surrounding cells. The potential change declined with distance from the current source as expected for two-dimensional current spread. The two-dimensional space constant (λ) was 770 μm for current flow in the circular direction and 177 μm for radial flow. The internal resistance of the epithelium (178–201 Ωcm) and the membrane time constant (5–10 ms) were direction independent. No propagated epithelial action potentials were observed.

3. Spontaneous miniature synaptic potentials of similar amplitude and rise-time were recorded intracellularly at distances of up to 1 mm from the motor giant axon. Ultrastructural evidence confirms that neuro-myoepithelial synapses also occur away from the giant axons. It is likely that synaptic sites are widespread in the myoepithelium, probably associated with the lateral motor neurones as well as the giant axons. Local stimulation of lateral motor neurones generally produced contraction in distinct fields. We suppose that stimulation of a single motor giant axon excites a whole population of lateral motor neurones and hence a broad area of the myoepithelium.

INTRODUCTION

Aglantha digitale is a hydrozoan medusa with a rapid escape swimming response which consists of multiple contractions of the entire bell-shaped subumbrellar muscle sheet or myoepithelium. This behaviour, which is unusual in jellyfish, can be

Key words: Coelenterate, neuromuscular transmission, epithelium.

attributed to the specialized neuromuscular organization in *Aglantha*. There are eight motor giant axons (~40 μm diameter) which run up the inside of the bell and which are excited in rapid succession when the medusa is stimulated mechanically (Singla, 1978; Donaldson, Mackie & Roberts, 1980; Roberts & Mackie, 1980). The motor giant axons provide a pathway for the rapid radial conduction of excitation and they make numerous synapses onto the myoepithelium. These synapses are unusual in that it is possible to record intracellularly at both pre- and postsynaptic sites.

In this paper we describe neuromuscular transmission at these giant motor axon to myoepithelial cell synapses during fast (escape) contraction and give details of the way in which excitation spreads between the motor giant axons. We present evidence for the participation of fine lateral motor neurones which appear to innervate the myoepithelium in distinct fields. Escape swimming can be attributed to the concerted action of the entire population of these neurones each of which produces the contraction of a small area of myoepithelium.

METHODS

Specimens of *Aglantha digitale* were taken from surface water at the dock of the Friday Harbor Laboratories, Washington, U.S.A., and kept in fresh flowing sea water at 12–15 °C for up to 3 days. Other experiments were carried out at the University of Victoria, British Columbia, Canada, and there the animals were, in most cases, caught locally using a 500-μm mesh net with a Reeve end. The net was pulled vertically from a depth of 120 m at a rate of approximately 6 m min^{-1}. Animals were transferred to sea water (taken from a depth of 100 m) and kept at 6 °C for periods of up to 3 days.

The experimental preparation consisted of a single bell, slit up one side and with the apex removed. In many experiments the margin (with the ring giant axon) was also removed and the preparation became a 'strip' of myoepithelium separated into octants by the motor giant axons. The myoepithelium was covered with sea water at 12–15 °C, illuminated from below and carefully pinned flat to a layer of Sylgard in a transparent dish with cactus (*Opuntia*) spines. Intracellular recording was carried out using 3 mol l^{-1} KCl-filled glass pipettes with resistances of 40–50 MΩ and individual axons were stimulated by using brief current pulses from a bipolar stainless-steel electrode. For intracellular current injection, thin-walled glass tubing was used to make 3 mol l^{-1} KCl-filled glass micropipettes with resistances of 10–15 MΩ. In many experiments the preparation was immobilized by adding $MgCl_2$ to the bathing medium. A solution containing 127 mmol l^{-1} Mg^{2+} was found to prevent contraction in *Aglantha* without significantly affecting the electrical activity associated with escape swimming recorded in either the motor giant axon or the nearby myoepithelium (Fig. 1). However 70 mmol l^{-1} Mg^{2+} does block low potential Ca^{2+} activation (associated with slow swimming; see Mackie & Meech, 1985) and so this is excluded from consideration here.

Anatomical observations were made on living tissue using a Zeiss microscope equipped with Normarski differential interference contrast optics and attached

camera lucida. For electron microscopy, medusae were immobilized in isotonic $MgCl_2$ ($67{\cdot}5\,g\,l^{-1}$) diluted with an equal volume of sea water. The material was fixed in 2·5% glutaraldehyde in $0{\cdot}4\,mol\,l^{-1}$ Millonig's phosphate buffer for 1 h at room temperature. It was rinsed in the same buffer, post-fixed in 1% osmium tetroxide in phosphate buffer for 1 h at 4 °C, dehydrated through a graded series of ethanol and propylene oxide and embedded in Epon 812. Thin sections were stained with uranyl acetate and lead citrate.

The lanthanum technique for gap junctions introduced by Revel & Karnovsky (1967) was modified to minimize swelling in *Aglantha*. The immobilized material was

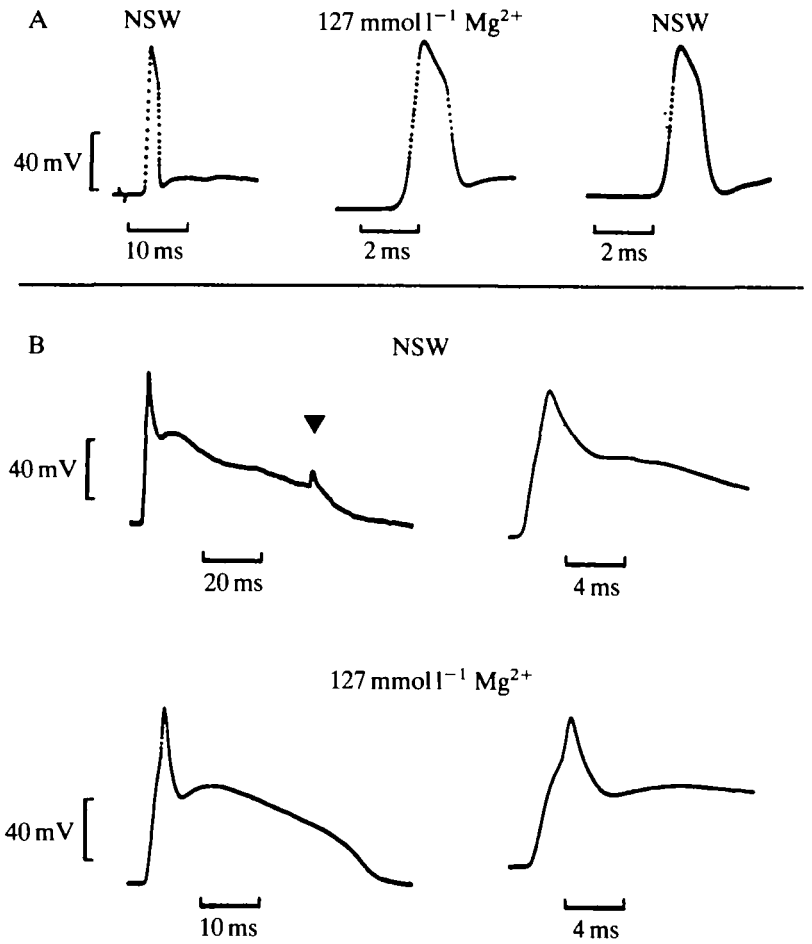

Fig. 1. Intracellular records from motor giant axon (A) and the nearby myoepithelium (B) to show the effect of 127 mmol l^{-1} Mg^{2+} sea water. External stimulation elicited an action potential in the motor giant axon and a postsynaptic potential in the myoepithelium. Note the prolonged depolarizing afterpotential which follows the axon spike in A and the muscle spike which rides on top of the postsynaptic potential in B. The myoepithelial response recorded in normal sea water (NSW) in B is more irregular than that recorded in high magnesium sea water because of contraction of the myoepithelium (arrowhead). The records have been retouched where necessary to show sharply rising and falling phases. Resting potentials: A, −56 mV, −66 mV, −55 mV; B, −68 mV, −78 mV, −86 mV, −74 mV.

fixed for 24 h at room temperature in a mixture containing 50 % glutaraldehyde, 1 part; 0·3 mol l^{-1} sodium chloride, 7 parts; 0·2 mol l^{-1} cacodylate buffer, 8 parts; 4 % colloidal lanthanum hydroxide (prepared from lanthanum nitrate, Revel & Karnovsky, 1967), 4 parts; and 55 mg calcium chloride per 100 ml of the fixative. This was followed by three rinses of 20 min each in a mixture of 0·6 mol l^{-1} sodium chloride, 3 parts; 0·2 mol l^{-1} cacodylate buffer, 3 parts; and 4 % colloidal lanthanum, 2 parts. The samples were post-fixed for 3 h at room temperature in a mixture of osmium tetroxide, 1 part; 0·2 mol l^{-1} cacodylate buffer, 2 parts; and 4 % colloidal lanthanum, 1 part. The material was rinsed as above, dehydrated up to 50 % ethanol and stained, *en bloc*, for 1 h at room temperature in a mixture containing absolute ethanol, 50 ml; double distilled water, 24 ml; 4 % colloidal lanthanum, 25 ml; and uranyl acetate, 1 gm. In all solutions 9 % sucrose was added to adjust the osmolarity. The material was dehydrated quickly through a series of ethanol and propylene oxide and embedded in Epon 812. Thin sections were studied with a Philips EM 300 electron microscope without staining.

RESULTS

Anatomy

The neuromuscular system of *Aglantha* has been studied by electron microscopy (Singla, 1978) and interference light microscopy of living specimens (Roberts &

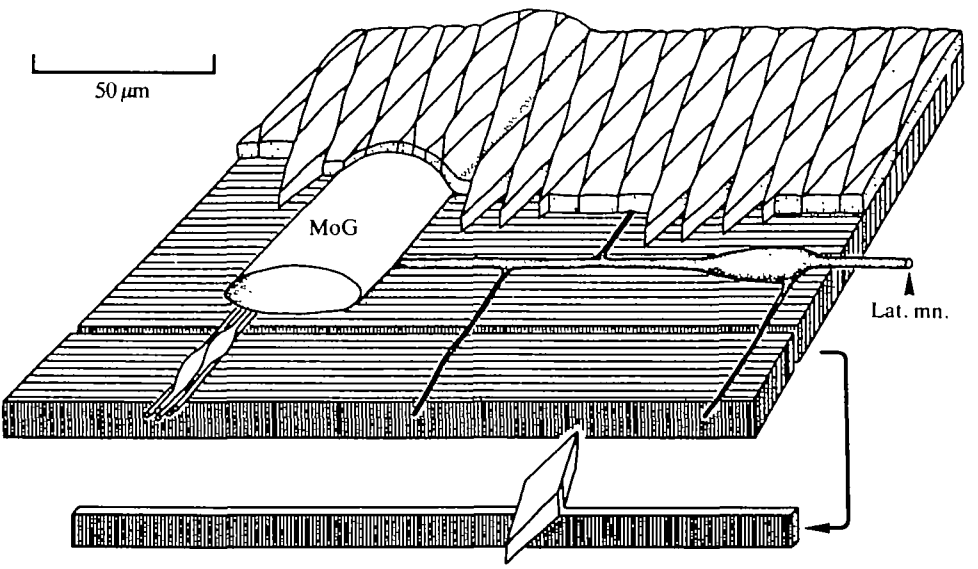

Fig. 2. Diagram of part of the subumbrella myoepithelium near a motor giant axon (MoG) which runs from the margin towards the apex of the bell (i.e. radially) over the muscle tails of the myoepithelial cells. The muscle tails run in a circular direction and are shown by the vertical striations. An isolated myoepithelial cell is shown at the bottom of the figure to clarify its structure. The cell body is elongated in the radial direction. A small bundle of fine axons with somata run parallel to the motor giant axon. The lateral motor neurone (Lat. mn.) has a principal circumferential axon (which makes contact with the motor giant axon) and finer radial branches. Its cell body is 100–500 μm from the motor giant axon.

Mackie, 1980). The main features of the region of the subumbrella around each motor giant axon are shown in Fig. 2. The subumbrella myoepithelium is one cell thick and made up of radially elongated cell bodies with underlying striated muscle tails oriented in a circular direction. In cells separated by maceration, muscle tails were 500–600 μm long. The myoepithelium is innervated by eight motor giant axons which run radially up the bell from the margin. Neuromuscular synapses occur along the whole length of these axons and make direct contact with the myoepithelial cells (Fig. 3A). Injection of Lucifer Yellow into individual giant axons has shown that they are dye coupled to lateral motor neurones (Weber, Singla & Kerfoot, 1982).

Lateral motor neurones (Figs 2 and 4) lie between the cell bodies and the muscle tails of the myoepithelium. In an animal with a bell height of 8·8 mm, lateral processes emerged from a motor giant at intervals ranging from 140–800 μm (mean, 350 μm) although some closer intervals were seen in other specimens. Lateral motor neurones have cell bodies which are 11–16 μm across and a principal axon 2–4 μm in diameter which runs from the motor giant axon in a direction parallel to the circular muscle tails. In a fresh preparation these axons could be traced for at least 1 mm across a 2 mm octant; occasionally they could be followed as far as, even beyond, the adjacent motor giant axon. In many preparations radial branches (1–2 μm in diameter) were visible (Fig. 4) and these ran approximately parallel to the motor giant axons for about 400 μm; they had a mean spacing of $137 \pm 69{\cdot}4$ μm (S.D.; $N = 25$). Some of the fine branches were near the resolution limit of the method. Other branches appeared to end abruptly but it is possible that they continued at a lower level. Examples of visible overlap between adjacent lateral neurones were common, particularly in the circular direction (Fig. 4B) but it is not known whether apparent contact sites correspond to transmission sites. Synapses between fine axons and myoepithelial cells were found well away from the motor giants (Fig. 3B) and we assume that the lateral motor neurones make multiple synapses onto the myoepithelial cells along their whole length.

Sections of myoepithelium prepared for electron microscopy showed junctions between the myoepithelial cell bodies (Fig. 5A). These myoepithelial junctions had a typical gap-junction structure when fixed in lanthanum-containing solution (Fig. 5B). There were also junctions between the motor giant axon and the myoepithelium (Fig. 3A) which were similar in appearance to the myoepithelial junctions but it was not possible to find whether they had a true gap-junction structure because lanthanum failed to penetrate beyond the myoepithelial layer. These findings are summarized in Table 1.

Physiology

Current spread in the myoepithelium

In *Aglantha* the myoepithelial cells are dye-coupled, and there are gap junctions between the cell bodies (Singla, 1978; and Fig. 5). Gap junctions are thought to be the site of a low resistance current pathway between cells (Barr, Dewey & Berger, 1965; Payton, Bennett & Pappas, 1969) and Fig. 6 shows that the cells are indeed electrically

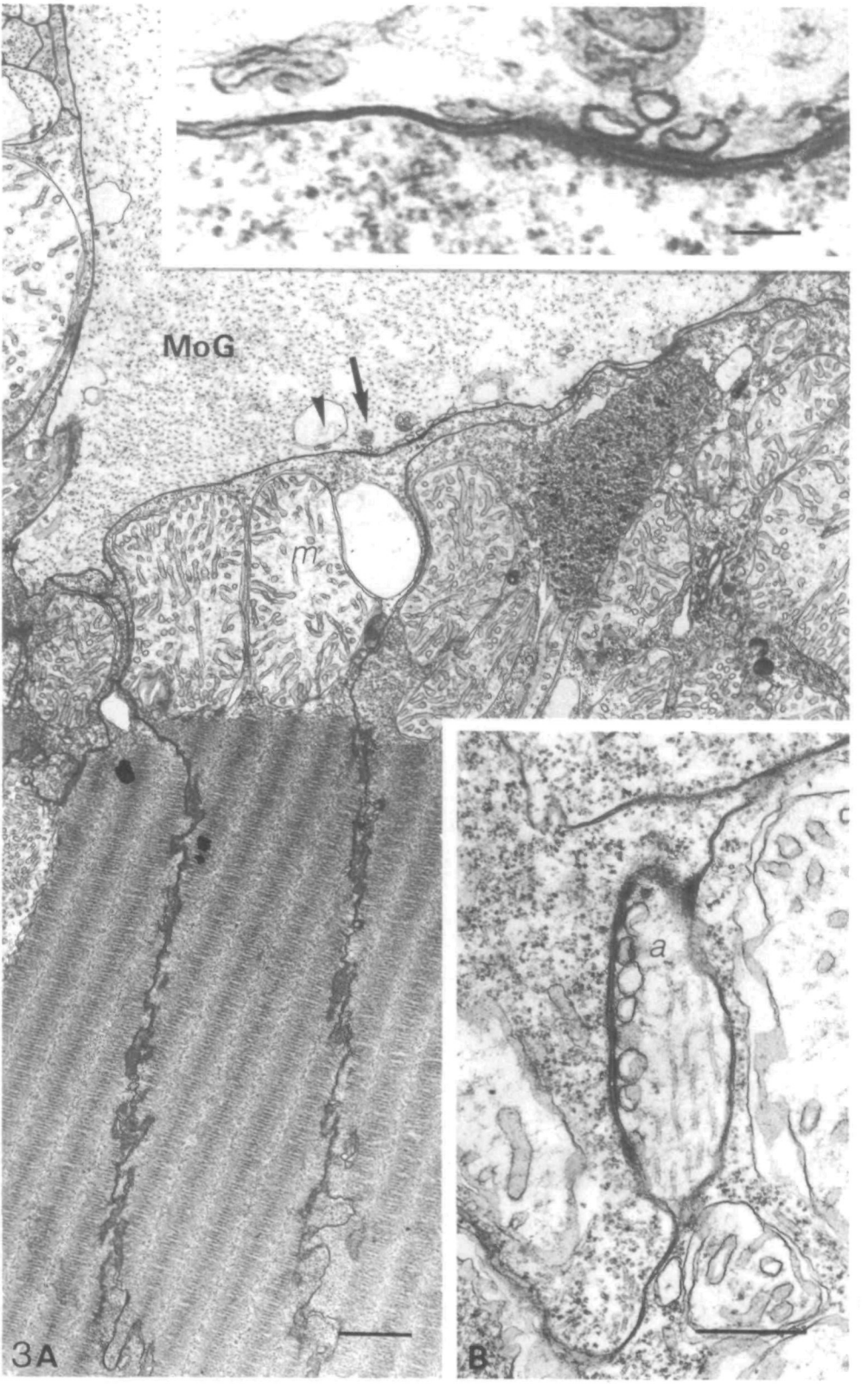
MoG
m
3A
a
B

coupled. Current injection into one cell produced a voltage change in surrounding cells which was a linear function of injected current over a wide range (Fig. 7).

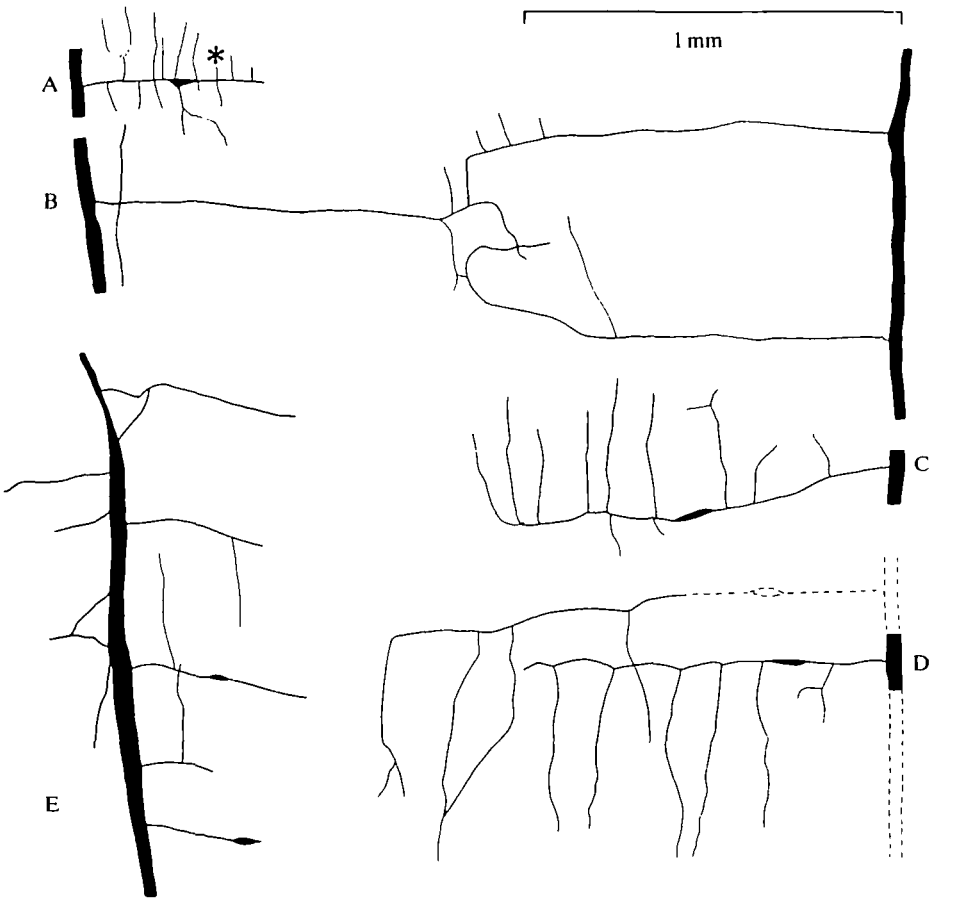

Fig. 4. *Camera lucida* drawings from living specimens showing lateral motor neurones and giant motor axons in the myoepithelium of the subumbrella. The motor giant axons run radially from the margin (bottom) towards the apex (top) and are usually about 2 mm apart. Drawings from different preparations (A to E) have been aligned as if they formed part of a single octant between two giant motor axons (large black profiles). (A) Part of a lateral motor neurone with an obvious soma and many radial branches (mean spacing 65 μm). Asterisk marks a radial axon from another lateral motor neurone. (B) Three lateral motor neurones, two of which show overlap of axons in the central region of the octant. Most of the radial branches and cell somata were omitted. (C) A lateral motor neurone with an obvious soma where all the radial branches were drawn. (D) Parts of two lateral motor neurones near the margin showing overlap of radial branches. The upper lateral motor neurone extends across the central region of the octant. (Dashed lines were not on the original drawing.) (E) Illustrates the way in which lateral motor neurones contact the giant motor neurone in the region near the apex. Radial branches omitted. Orientation: radial (up-down), circular (left-right).

Fig. 3. (A) Junctions made by a motor giant axon (MoG) onto a neighbouring myoepithelial cell with large mitochondria (*m*) and striated muscle tail. A gap junction (arrowhead) lies close to a conventional vesicular synapse (arrow). Inset shows this area at higher magnification. Scale bar, 1 μm; inset, 0·1 μm. (B) A neuromuscular synapse from a lateral neurone (*a*) onto a myoepithelial cell. Scale bar, 0·5 μm.

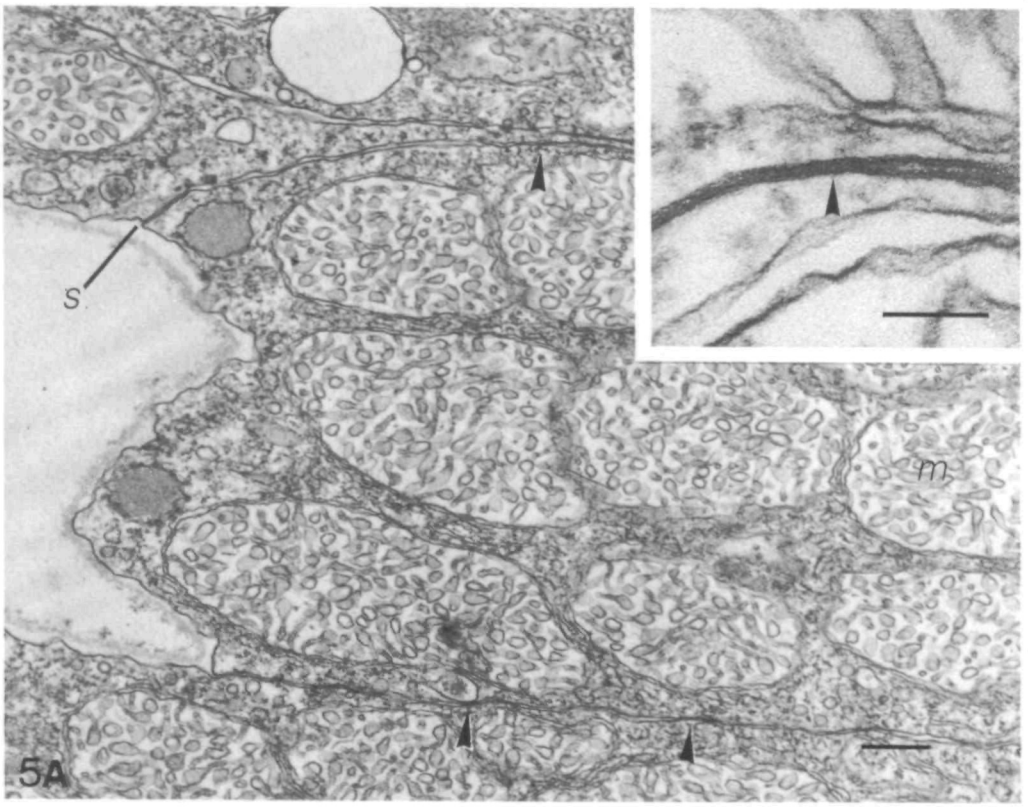
S
m
5A

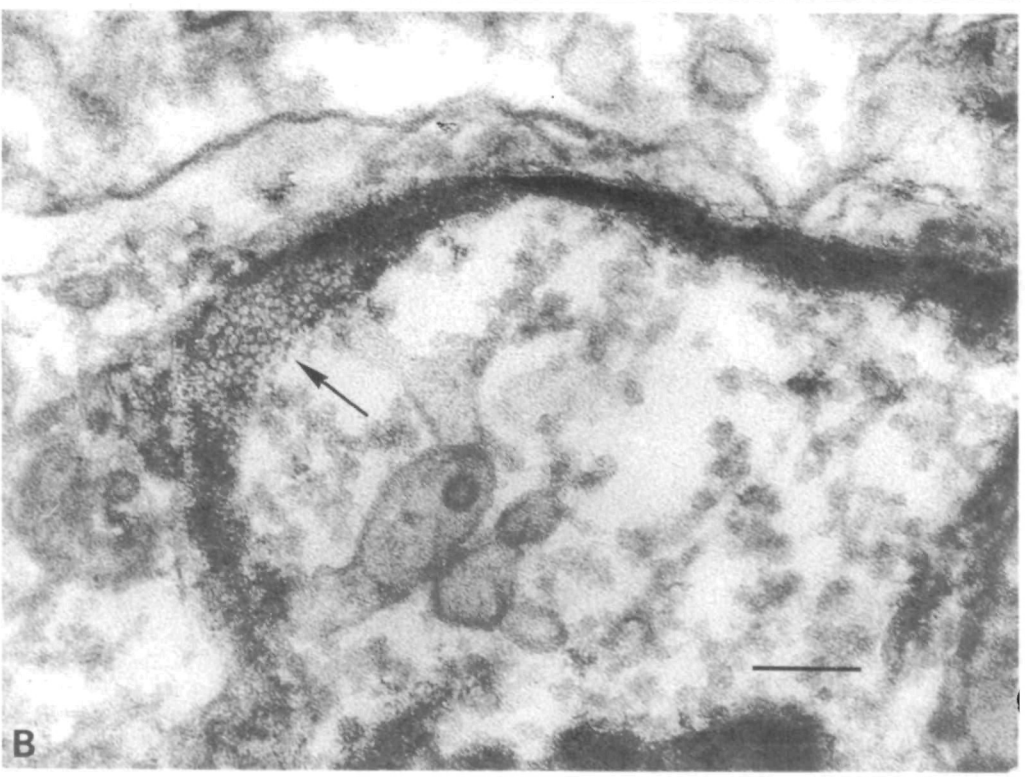
B

Table 1. *Summary of synaptic connections between neuronal and myoepithelial elements discussed in the text*

Junction	Chemical synapse		Electrical synapse		
	Structural evidence	Electrophysiological evidence	Dye coupling	Gap junction	Electrophysiological evidence
Giant axon/ myoepithelium	+	+		+	–
Giant axon/lateral motor neurone			+		+
Lateral motor neurones/ myoepithelium	+	+			
Lateral motor neurone/ lateral motor neurone		+			
Myoepithelial cell/ myoepithelial cell			+	+	+

In a thin sheet of coupled cells current flow is restricted to two dimensions and the steady-state change in membrane potential declines with distance from a point current source as a modified Bessel function (Woodbury & Crill, 1961; Eisenberg & Johnson, 1970; Shiba, 1971; Frömter, 1972; Jack, Noble & Tsien, 1975).

i.e.

$$V = \frac{I_o r_x}{2\pi} \cdot K_o\,(x/\lambda_2), \tag{1}$$

where V is the change in membrane potential (volts); I_o is the amplitude of the injected current (amperes); $K_o\,(x/\lambda_2)$ is a modified Bessel function of zero order with the argument (x/λ_2) and values of K_o taken from Abramowitz & Stegun (1965); x is the distance between the recording site and the current source (cm); λ_2 is a two-dimensional space constant defined as $(R_z/r_x)^{1/2}$ where R_z is the egress resistivity from the cytoplasm (Ωcm^2); r_x is the resistance of unit length and breadth of the epithelial interior (Ω).

$$r_x = R_i/d, \tag{2}$$

where R_i is the resistivity of the epithelial interior (Ωcm) and d is the thickness of the epithelium (cm).

The intracellularly recorded potential change declined with distance from the current source (Fig. 8) as expected for two-dimensional current spread but, unlike the simple epithelium of *Euphysa* (Josephson & Schwab, 1979), the sheet did not behave as if it were radially symmetrical about the point of injection. The current was found

Fig. 5. (A) Superficial area of subumbrellar myoepithelium (subumbrellar cavity to left). Parts of four cells can be seen. The outer ends of intercellular clefts are sealed by septate junctions (*s*). Elsewhere gap junctions occur between neighbouring cells (arrowheads, and inset). *m*, mitochondrion. Scale bar, 0·5 μm; inset, 0·1 μm. (B) Tangential section of gap junction (arrow) between two myoepithelial cells with lanthanum staining the extracellular space. Scale bar, 0·1 μm.

to spread further in the circular direction than it did radially. The sheet can be treated as if it were isotropic if the distance scale is made a function of the angle formed with the fibre axis (Jack *et al.* 1975).

The values of λ_2 and R_i derived from the data by the method of Josephson & Schwab (1979) were: for circular current flow, $\lambda_2 = 770\,\mu m$, $R_i = 201\,\Omega cm$, and for radial current flow, $\lambda_2 = 177\,\mu m$ and $R_i = 178\,\Omega cm$. The myoepithelium was taken to be $10\,\mu m$ thick (Singla, 1978). These values were substituted in equation 1 to produce the solid lines shown in Fig. 8. The fit to the experimental points was sufficient for present purposes.

The myoepithelium in *Aglantha* is divided by the motor giant axons into octants. The myoepithelial cells that cover each giant axon are thinner than those in the main body of the epithelium (Singla, 1978) but we found no significant difference in either R_i or λ_2 (not shown).

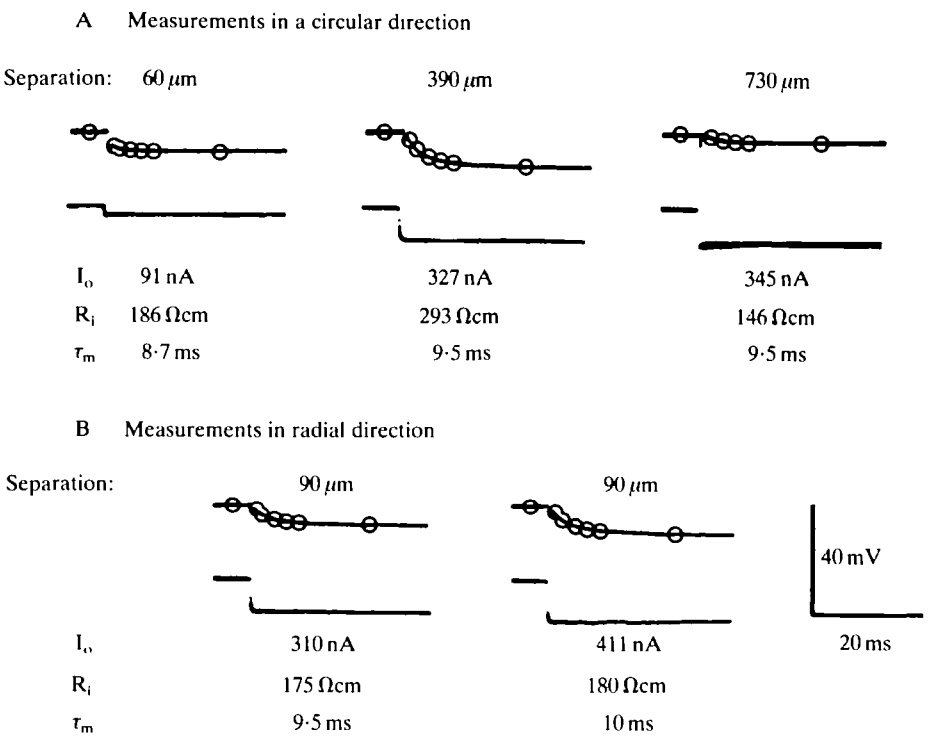

Fig. 6. Effect of hyperpolarizing current pulses (bottom traces) on the membrane potential (top traces) at different sites in the myoepithelium. The separation between the current injection and recording sites is shown. Measurements were made in both a circular (A) and a radial direction (B). I_o is the current intensity, R_i is the internal resistivity of the epithelium and τ_m is the time constant of the membrane derived by fitting equation 3 (open circles). Bathing medium: 70 mmol l^{-1} Mg^{2+} sea water. Resting potentials: 60 μm circular, −80 mV; 390 μm circular, −80 mV; 730 μm circular, −70 mV; 90 μm radial, −79 mV (both from same penetration).

There are two main difficulties in interpreting these results. First, gap junctions have been found only between epithelial cell bodies and not between muscle tails (Singla, 1978). Second, the method underestimates the total membrane surface encountered by the current and so it cannot be used to provide a measure of membrane resistance.

Membrane time constant

The transient response of a two-dimensional sheet to a maintained step change in current has been derived by Jack *et al.* (1975; page 88):

$$V = \frac{R_i I_o}{2\pi d} \int_o^T \frac{1}{2t} \exp\left(-\frac{R^2}{4t} - t\right) dt, \tag{3}$$

where $R = (x/\lambda_2)$ and $T = (t/\tau_m)$. τ_m is the time constant of the membrane; t is the time after the beginning of the step.

This expression was evaluated for us by Dr P. A. McNaughton using the NAG subroutine DO1AGF (Mark 8 release, Numerical Algorithms Group, Nottingham). The best fit to the experimental results was obtained with values of 5–10 ms for τ_m (Fig. 6, Table 2).

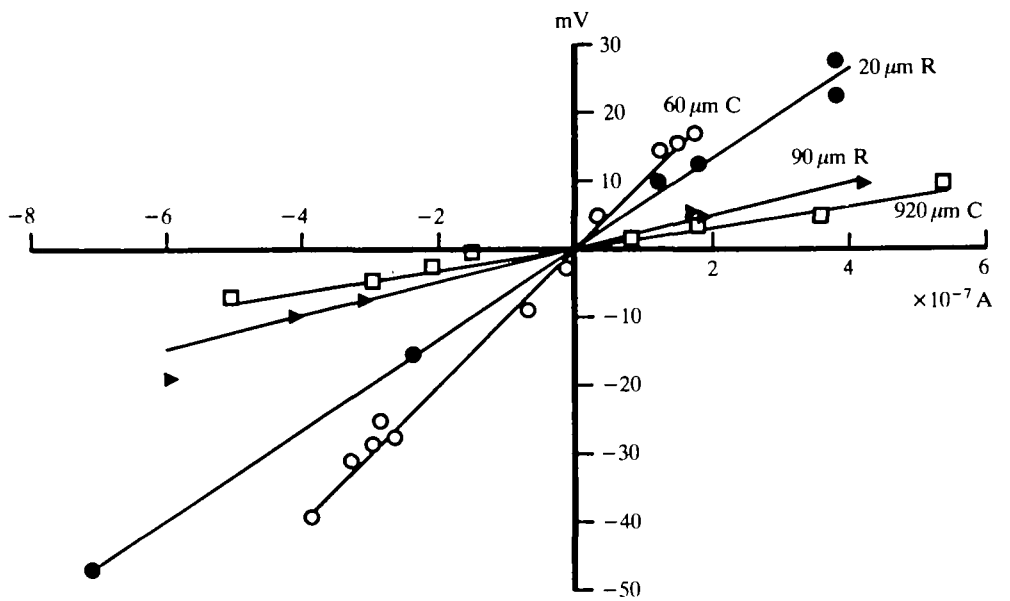

Fig. 7. Relationship between injected current and membrane potential at different locations in the myoepithelium. Abscissa: injected current. Ordinate: change in membrane potential. Orientation of current injection and membrane potential recording sites was radial (R, closed symbols) or circumferential (C, open symbols). Separation of the sites was 20 μm (closed circles), 90 μm (closed triangles), 60 μm (open circles) or 920 μm (open squares). The straight lines were drawn by eye. Bathing medium: 70 mmol l^{-1} Mg^{2+} sea water. Resting potentials: 20 μm radial, −75 mV; 90 μm radial, −79 mV; 60 μm circular, −80 mV; 920 μm circular, −75 mV.

Since τ_m was independent both of the orientation of the recording and injection sites and of the distance between them it can be used to provide an estimate of membrane resistance. If the membrane capacitance is $1\,\mu F\,cm^{-2}$, as it is for other biological membranes (Cole, 1968), and the two surfaces of the thin sheet are taken to have identical properties, the membrane resistance becomes 5000–10000 Ωcm^2 and λ_2 is 0·11–0·17 cm. This is close to the value of λ_2 measured in the circular direction under steady-state conditions but differs from that in the radial direction by a factor of six or more. The direction dependence of λ_2 measured under steady-state conditions can be accounted for if the current pathway is greater in the radial direction (see Woodbury, 1962). This means that the current must flow by an indirect route such that its pathway is six times longer than it appears to be from measurements on the surface.

However, Eisenberg & Johnson (1970) have provided a solution for the potential at any point in a two-sided slab. Their solution has two terms. The second term is independent of membrane properties and can be neglected because the myoepithelium is so thin; the dominant term differs from the solution given by Jack *et al.* (1975) and others by a factor of $\sqrt{2}$ in the argument of the Bessel function. This

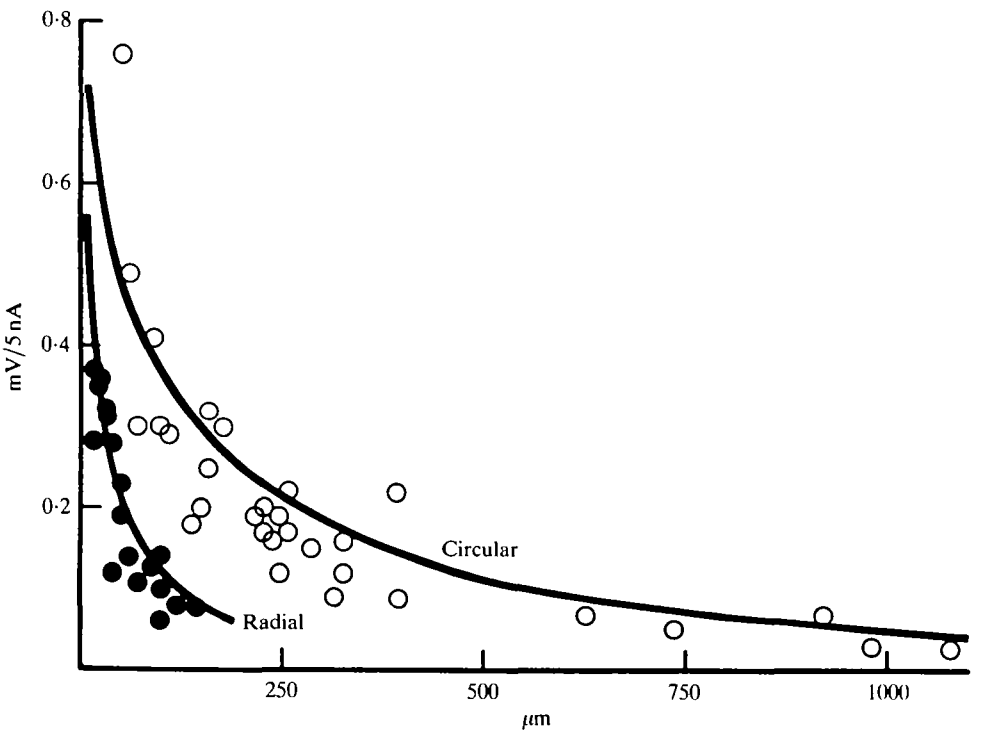

Fig. 8. Spread of current in the myoepithelium. Ordinate: mean membrane potential displacement produced by current injected at different distances from the recording site (abscissa). Open circles: measurements in a circular direction; closed circles: measurements in a radial direction. The solid line was calculated from equation 1 using $\lambda_2 = 770\,\mu m$ and $R_i = 201\,\Omega cm$ for current flow in a circular direction and $\lambda_2 = 177\,\mu m$ and $R_i = 178\,\Omega cm$ for current flow in a radial direction. Bathing medium; 70 mmol l^{-1} Mg^{2+} sea water.

means that the value of λ_2 in the circular direction becomes 0·11 cm; λ_2 in the radial direction becomes 0·03 cm.

Response of the myoepithelium to nerve stimulation

In *Aglantha*, stimulation of a single motor giant axon produced contraction throughout the bell of the animal. Intracellular records from the myoepithelium on the inner surface of the bell showed that contraction was preceded by a complex electrical response which resembled the end-plate potential at the frog neuromuscular junction (Fatt & Katz, 1951). The response consisted of a foot, a sharply rising phase, a shoulder, an overshooting spike-like component and a long phase of repolarization (Fig. 1). In frog the muscle response becomes a simple conducted action potential as it moves away from the neuromuscular junction but in *Aglantha* the myoepithelial response was dominated by the postsynaptic potential irrespective of the location.

Synaptic delay

The 'synaptic delay' associated with chemical transmission is defined by Katz & Miledi (1965*a*) as the time between the peak of the presynaptic spike obtained by focal external recording and the onset of the postsynaptic response. In the frog neuromuscular junction the synaptic delay as defined is 1 ms at 12 °C (see Katz & Miledi, 1965*b*; Fig. 4) while in the squid giant synapse the synaptic delay measured from the peak of the internally-recorded spike is about 1·4 ms at the same temperature (calculated from Lester, 1970; see also Takeuchi & Takeuchi, 1962; Bloedel, Gage, Llinás & Quastel, 1966). At another neuromuscular junction, in the coelenterate

Table 2. *Spread of current in the myoepithelium; time constant (τ_m) of myoepithelial cell membrane derived by fitting equation 3 to experimental data*

Direction of measurement	I_o (nA)	D/H	x (μm)	R_i (cm)	τ_m (ms)
Circular	208	H	46	254	5·5
Circular	262	H	59	246	5·8
Circular	91	H	59	186	8·7
Circular	196	H	154	160	5·1
Circular	138	D	254	150	9·5
Circular	153	H	254	210	9·5
Circular	327	H	393	293	9·5
Circular	345	H	732	146	9·5
Circular	182	H	924	236	5·8
Average circular $N = 9$				212 ± 48 (S.D.)	7·7 ± 2·0 (S.D.)
Radial	255	H	16	176	5·8
Radial	255	H	50	162	6·5
Radial	411	H	89	180	10·0
Radial	310	H	89	175	9·5
Average radial $N = 4$				173 ± 8 (S.D.)	8·0 ± 2·1 (S.D.)

I_o is the injected depolarizing (D) or hyperpolarizing (H) current.
x is the distance between injection and recording sites.
R_i is the internal resistance.

Polyorchis, Spencer (1982) has reported synaptic delays ranging from 0·9 to 7 ms with a mean at 3·2 ms ($N = 103$; temperature 14–19 °C).

In *Aglantha*, the synaptic delay measured from the peak of the internally-recorded axon spike at 12 °C was $0{\cdot}7 \pm 0{\cdot}1$ ms, (S.D.; $N = 6$) for recording sites in the myoepithelium 40–130 μm from the motor giant axon. Fig. 9 shows simultaneous intracellular records from the motor giant axon and from the myoepithelium 80 μm (A) and 600 μm (B) away. The delay increased progressively as the distance between the recording sites was increased. The electrical characteristics of the myoepithelium revealed by the current injection experiments (Fig. 8) suggest that very little current

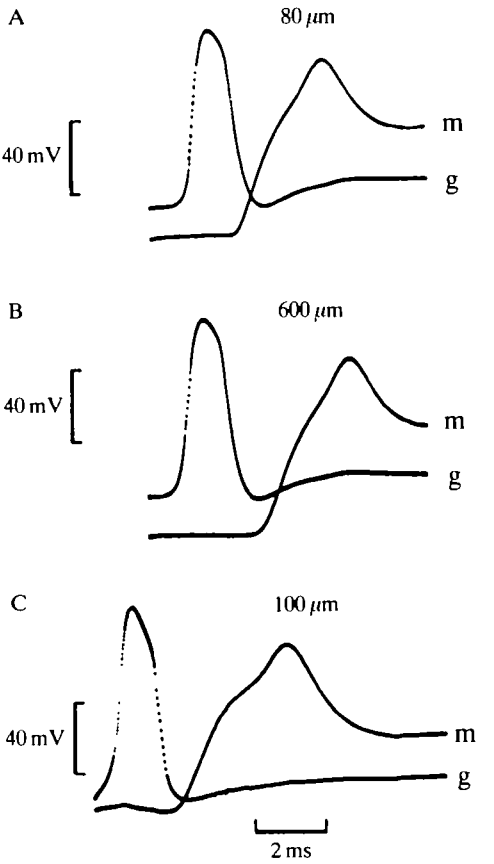

Fig. 9. Simultaneous intracellular records from motor giant axon (g) and nearby myoepithelial cell (m) following external stimulation of the giant motor neurone. Records A and B are from a single penetration of the axon and two separate penetrations of the myoepithelium, 80 μm (A) and 600 μm (B) from the recording site in the axon. Record C is taken from a different experiment: a circle (250 μm diameter) was scored in a region of the myoepithelium which included the motor giant. The axon and a nearby myoepithelial cell (separation 100 μm) were penetrated within this isolated region. The records were retouched where necessary to show the rising and falling phases of the axon spike. Bathing medium: 90 mmol l^{-1} Mg^{2+} sea water. Resting potentials: axon A −62 mV, B −65 mV, C −60 mV; myoepithelium A −77 mV, B −86 mV, C −67 mV.

should spread electrotonically from a point on the axon to a point in the myoepithelium as far as 600 μm away. This means that the postsynaptic event must be derived from some local synapse, probably on the lateral motor nerve, and that the delay includes the time taken for excitation to spread from the giant axon to the lateral nerve.

Other neuromuscular synapses along the motor giant axon are unlikely to contribute to the electrical response recorded in the myoepithelium in Fig. 9 unless they are within about 100 μm. Nevertheless we wanted to exclude the possibility of a contribution from synapses outside this range and so the experiment was repeated in a region of the myoepithelium isolated from the rest. An unfilled glass micropipette was used to sever muscle cells in a semi-circle on either side of the motor giant axon and the cells under the axon itself were carefully destroyed leaving the axon intact. Fig. 9C shows that the synaptic delay at the centre of an isolated area of myoepithelium 250 μm in radius was 0·8 ms. The experiment was repeated three times with similar results. The position of the synapse is unknown but it must be within the 500 μm length of axon that crosses the isolated area of epithelium. Action potentials in the motor giant axon travel 250 μm in about 0·05 ms (Roberts & Mackie, 1980) and so the measurement of synaptic delay must have an error of less than 10 %.

Current injection

A number of fine axons run alongside the motor giant axon (Fig. 2) and it is possible that they too are excited by the method of external stimulation used. To avoid this, current was injected directly into the motor giant axon. In five out of 11 preparations the myoepithelium responded in an all-or-nothing fashion (Fig. 10A) and in one of these preparations an intracellular record confirmed that the current levels used were sufficient to initiate an action potential (not shown).

In six preparations injection of current into the motor giant axon produced graded responses in the myoepithelium. In Fig. 10B the 1-ms current pulses were 10–100 nA but in other experiments with more prolonged pulses graded responses were produced by even smaller currents. It is likely that when the current electrode was near a synapse a local depolarization caused transmitter release without generating an axon spike.

Calcium contribution to neuromuscular transmission

In *Aglantha* external calcium ions were necessary for both neuromuscular transmission and for contraction. If calcium ions were added back to a calcium-free medium a graded postsynaptic potential appeared which increased in size and eventually developed a spike-like component. The appearance of the muscle spike coincided with the appearance of contraction in the myoepithelium. If we assume, as seems likely, that calcium influx is necessary for contraction it suggests that an inward calcium current contributes to the spike but not to the postsynaptic potential. Abolition of the postsynaptic potential in Ca^{2+}-free medium can therefore be attributed to a failure in neuromuscular transmission as it is in the frog (Katz & Miledi, 1965*c*).

Miniature synaptic potentials

Events which probably represent spontaneous release of transmitter at neuromuscular synapses may be recorded from different sites in the myoepithelium. Fig. 11 shows examples recorded at an intracellular site within 20 μm of the motor giant axon (A) and at a distance of about 1 mm (B). We assume that these events are miniature postsynaptic potentials but can provide no pharmacological evidence for this because the synaptic transmitter is as yet unidentified. In general the postsynaptic potential recorded after an action potential in the motor giant axon had a longer duration

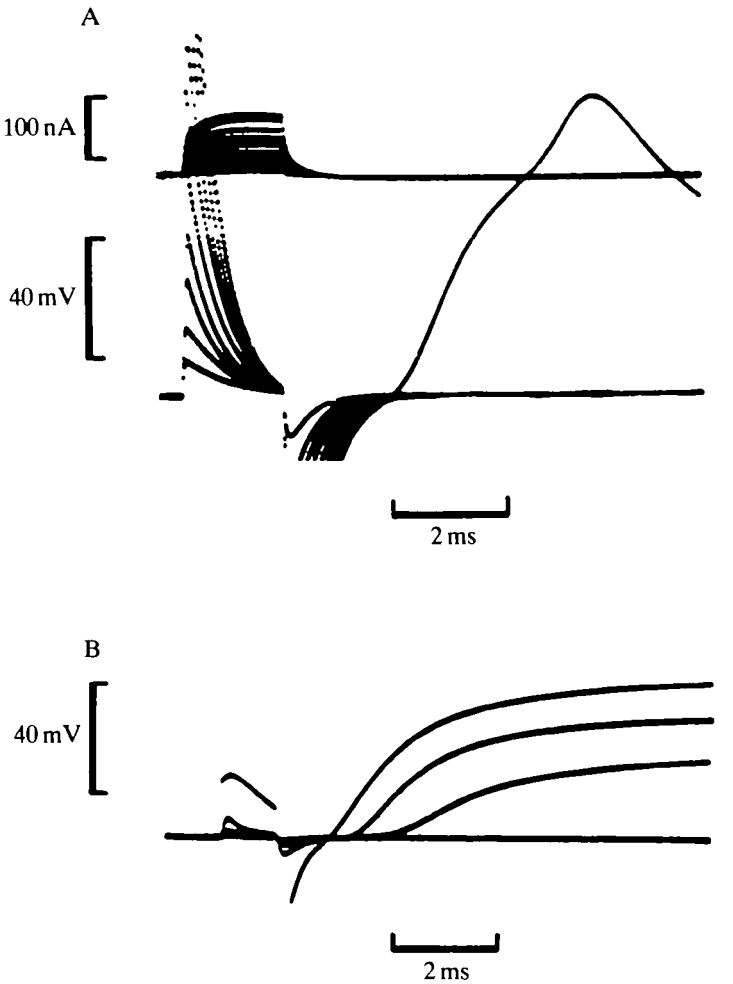

Fig. 10. Current injection into motor giant axon. A brief (1·75 ms) just suprathreshold depolarizing current pulse (top trace) produced a delayed depolarization of the myoepithelium (bottom trace). Bathing medium, normal sea water, resting potential, −78 mV. Graded responses were sometimes seen, as in B; recording conditions as in A but with 1-ms pulse and without the current trace. Four superimposed traces. Micropipette separation: 100 μm, bathing medium, 90 mmol l^{-1} Mg^{2+} sea water; resting potential, axon −63 mV, myoepithelium, −74 mV.

than the miniature events but this may be because of contributions from synapses on either side of the octant. The complex shape of the miniature potentials may also be because more than one synapse contributes to each event. The main point here is that spontaneous miniature potentials of similar amplitude and rise time may be recorded at different distances from the motor giant axon as if there are synaptic sites throughout the myoepithelium. These synapses are in addition to those from the giant motor axons and are possibly associated with the lateral motor neurones (see also Fig. 3B).

Lateral motor neurones

Stimulation of the inside surface of the bell at certain locations produced a contraction which was restricted to a patch of myoepithelium around the stimulating electrode and which usually spread about half-way across the octant. The most effective stimulation sites were found to lie along a central line within any one such area (Fig. 12). Contraction failed if the myoepithelium was stimulated outside the area. In some preparations we were able to see the lateral motor neurones with a dissecting microscope so that they could be stimulated directly. The contraction which resulted was generally restricted to the same roughly rectangular region of myoepithelium covered by the visible branches of the lateral motor neurone. Repetitive stimuli sometimes produced contractions not only in the muscle field surrounding the stimulated neurone, but also in fields apparently innervated by neighbouring lateral neurones. After the addition of isotonic Mg^{2+} the contraction

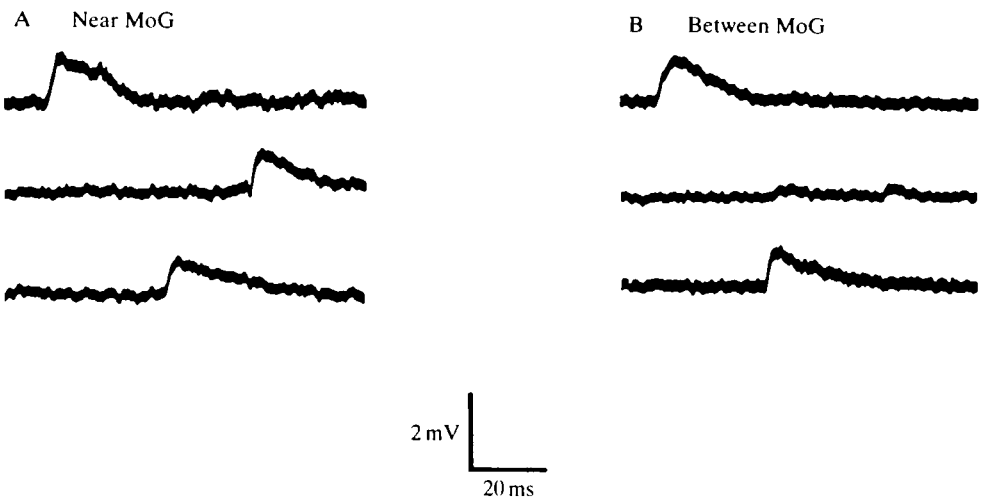

Fig. 11. Intracellularly recorded spontaneous electrical activity from the myoepithelium. (A) Recording site within 20 μm of the motor giant axon; (B) recording site mid-way between two motor giant axons. Bathing medium, normal sea water; resting potential, −83 mV.

was confined to the field of the stimulated neurone. This suggests that when stimulated, individual lateral motor neurones can elicit contraction in a well-defined area of the myoepithelium and that excitation can spread between lateral neurones *via* Mg^{2+}-sensitive synapses.

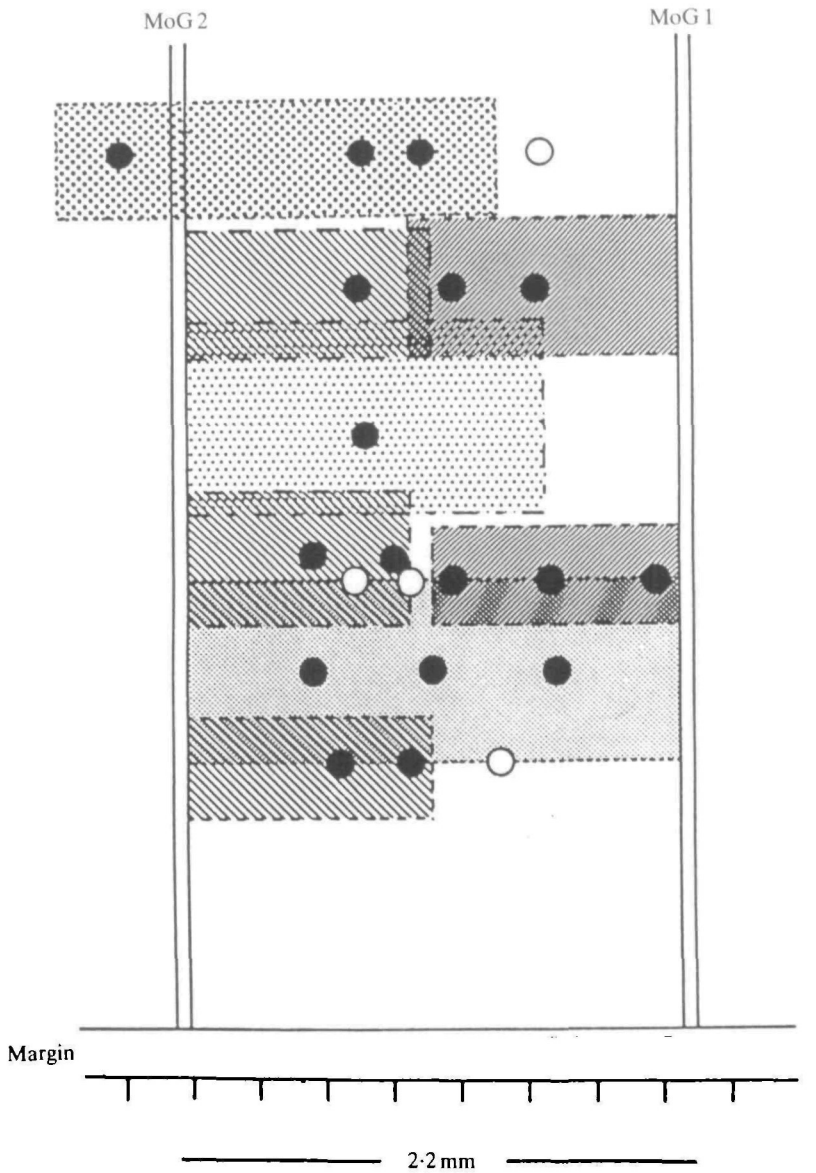

Fig. 12. Areas of myoepithelium that contract in response to focal external stimulation (1 ms current pulses). Filled circles show some of the locations where threshold stimulation evoked contraction in the surrounding approximately-rectangular area, shown with one style of texturing. Open circles show some ineffective stimulus locations where contraction was confined to the region under the stimulating electrode.

Conduction through the myoepithelium

To investigate the circular spread of excitation, the electrical events recorded from different parts of the myoepithelium were carefully compared. The postsynaptic

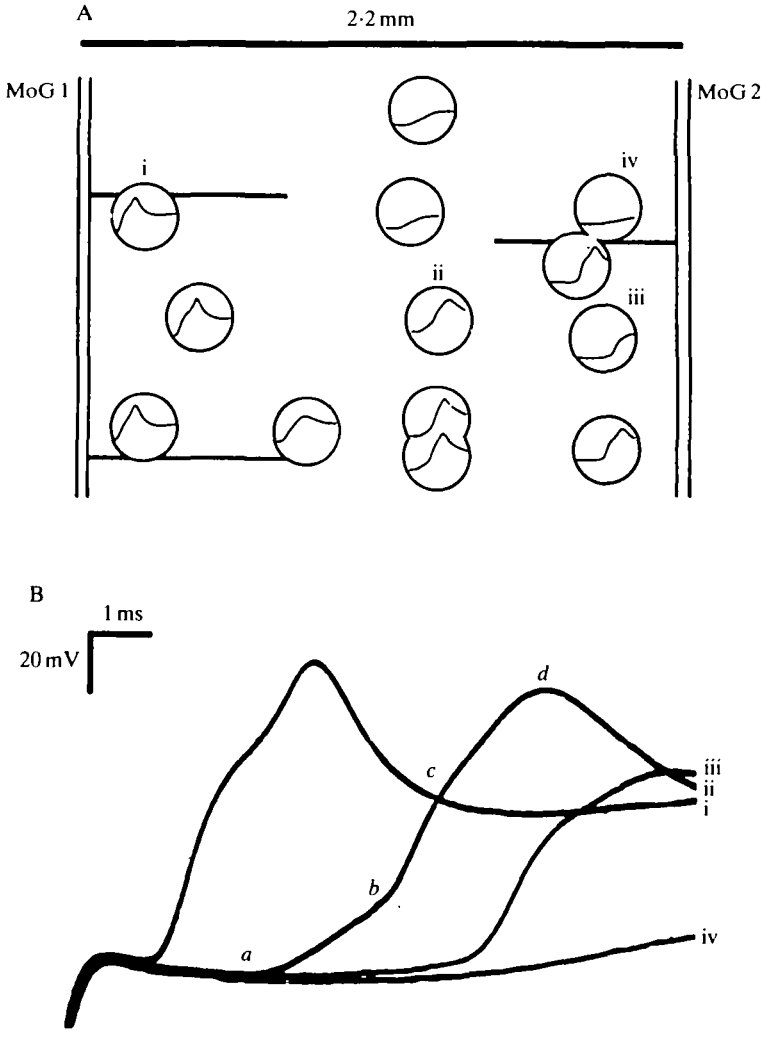

Fig. 13. Spread of excitation across an octant. (A) Diagram of the region between two motor giant axons (MoG 1, MoG 2) showing the position of three lateral motor neurones visible under Nomarski optics (thick lines) and the positions of 13 intracellular recording sites across the myoepithelium. The potential change shown was recorded at each site following external stimulation of MoG 1 (scale as for B÷8·8). Bathing medium, normal sea water. (B) Four superimposed records (from A) showing the postsynaptic potential at different sites in the myoepithelium. The records were (i) 0·2 mm (resting potential, RP −76 mV); (ii) 1·3 mm (RP −76 mV); (iii) 1·9 mm (RP −76 mV) and (iv) 1·9 mm (RP −72 mV) from the stimulated giant axon. Record (ii) from midway between the two motor giant axons had three distinct components: *a–b*, the foot; *b–c*, the postsynaptic potential; *c–d*, the active response. All three components may also be recognized in record (iii) although the foot is less pronounced. A significant foot is absent from record (i).

response recorded from a strip preparation following the stimulation of a single motor giant axon was generally of a uniform peak amplitude at sites many millimetres apart but there were significant differences in the overall shape. At the centre of the octant the response appeared to have three components; a 'foot' (*a–b* in Fig. 13B), which we take to be a postsynaptic event which has spread electrotonically from an area of myoepithelium near the stimulated motor giant axon, a postsynaptic potential (*b–c* in Fig. 13B) initiated near the recording site and an active response (*c–d* in Fig. 13B). On the far side of the octant the electrotonic component is small and the postsynaptic potential rises sharply. Nearer the stimulated motor giant axon an electrotonic component from the far side has the effect of prolonging the muscle response.

In Fig. 13A the postsynaptic response of the myoepithelium was recorded at 13 different sites in a single octant. The positions of three lateral motor nerves visible under Normarski optics are also shown. It seems that the presence of a visible lateral motor nerve in the region of the recording site did not always mean that the postsynaptic potential would be full-sized. Likewise a region in which no lateral motor nerve was visible sometimes had a pronounced postsynaptic potential and muscle spike. This suggests that the synapses may be associated with radial processes of the lateral motor neurones that were beyond the resolution of our microscope.

The muscle-spike was absent from some sites in the myoepithelium, and as shown in Fig. 13 (sites iii & iv), these postsynaptic responses were graded in amplitude as though they were derived from the electrotonic spread of current from a synaptic region nearer to the stimulated motor giant axon. In this experimental situation the spread of current will be confined to the lateral direction (the myoepithelial cells on either side having been uniformly depolarized). Hence the tissue should behave as a two-dimensional cable with a linear current source and the postsynaptic potential should decrease in an exponential fashion across the octant:

$$V = V_0 e^{x/\lambda_2}. \tag{4}$$

Graded myoepithelial responses were recorded from three different preparations at different distances from a stimulated motor giant axon. As Fig. 14 shows, the data are well fitted by equation 4 ($\lambda_2 = 770\,\mu$m) for distances greater than about 800 μm from the motor giant axon. For distances less than 800 μm the myoepithelial response was relatively constant. This result could be accounted for if synapses between the lateral motor neurones and the myoepithelium were confined to the region up to 800 μm from the motor giant axon and the response of the myoepithelium outside this area consisted of electrotonic spread from the synaptic region.

Although as we have seen, graded responses were sometimes recorded from the myoepithelium it was not uncommon to find a full-sized postsynaptic potential with its associated muscle spike even in regions of the octant some distance away from the stimulated motor giant axon. This suggests that impulses in the lateral motor nerves propagate across the octant. To determine whether the spread of contraction was associated with electrical activity in other giant motor axons we used a strip preparation and recorded intracellularly from the giant axon on the far side of the

octant. Fig. 15 shows the potential change recorded in one giant motor axon when an adjacent motor giant axon was stimulated. Care was taken to abolish all movement by using sea water containing 127–150 mmol l^{-1} $MgCl_2$. Events of a similar amplitude (10–15 mV) were recorded at different sites along the axon. At each site the recorded events were entirely reproducible but at different sites there was considerable variability in shape. Fig. 15 shows that the postsynaptic potential recorded in the nearby myoepithelium arises about 1 ms after the start of the event recorded in the giant motor axon and so it seems that the spread of excitation in the myoepithelium follows the spread of excitation to the giant motor axon. We assume that these events represent the summed activity of lateral neurones which spreads into the motor giant by way of electrical junctions.

Under the electron microscope, structures are frequently seen which appear to be gap junctions between the motor giant axon and the myoepithelium (see for example Fig. 3A) and so we tested the possibility that the nerves and muscles are electrically coupled. On three occasions a small (3 mV) depolarization was recorded in the myoepithelium coincident with an action potential in the nearby motor giant axon but generally action potentials in the axon were not visible at recording sites in the myoepithelium. Furthermore stimulation of a single lateral motor neurone produced only a relatively brief event in the motor giant axon in spite of widespread and prolonged depolarization of the surrounding myoepithelium. Consequently we think that significant electrical coupling between the motor giant axon and the myoepithelium is unlikely.

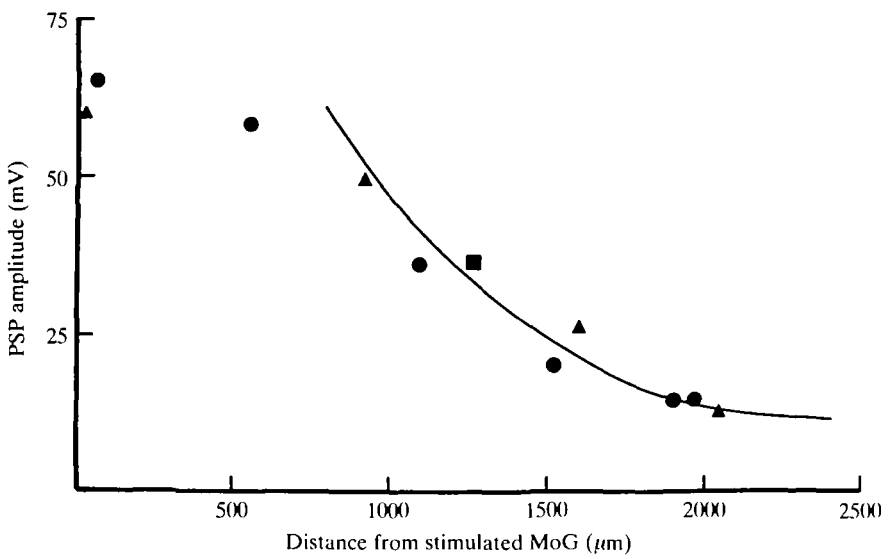

Fig. 14. Amplitude of the postsynaptic potential (PSP) at different distances from an externally-stimulated motor giant axon (MoG). Three preparations (different symbols) in which the spike component of the myoepithelial response was absent. The solid line was calculated from equation 4 using $\lambda_2 = 770\,\mu m$. Bathing medium, 90 mmol l^{-1} Mg^{2+} sea water (triangles); 127 mmol l^{-1} Mg^{2+} sea water (circles); normal sea water (squares).

DISCUSSION

Electrical characteristics of the myoepithelium

The myoepithelium of the hydrozoan medusa *Aglantha digitale* is a thin sheet of electrically coupled cells. Current from a point source is restricted to two dimensions but spreads further around the bell of the animal than it does radially. Other characteristics of the sheet, its time constant and its internal resistance, are independent of direction and we suppose that the anisotropicity arises from the current path length. The path length may depend on the number and distribution of operative gap-junctions (see Detwiler & Hodgkin, 1979), which we assume to provide the low resistance pathway between the cells (Fig. 5). The difference between the space constant derived from steady-state measurements and that calculated from the membrane time constant probably arises because of differences between the effective membrane area and the surface area. It may be, at least in part, the result of an extended path length. The internal resistance (178–201 Ωcm at 12–15 °C) is independent of path length and is similar to that found for the exumbrellar epithelium of the hydromedusa, *Euphysa japonica* (196 Ωcm at 9–11 °C; Josephson & Schwab, 1979) and that found for the giant smooth muscle cells of the ctenophore *Beroë* (154 Ωcm at 20–22 °C; Hernandez-Nicaise, Mackie & Meech, 1980). A value of

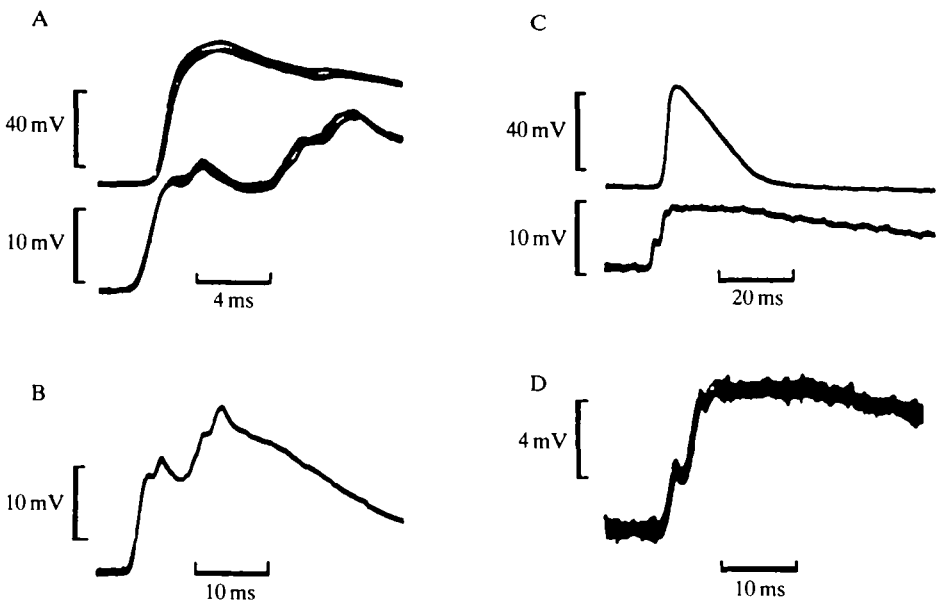

Fig. 15. Intracellular potential change in a motor giant axon after external stimulation of an adjacent motor giant axon. (A) Simultaneous records from motor giant axon (bottom) and nearby myoepithelium (top). Three superimposed traces. (B) Single trace from motor giant axon, same location as A. (C) As A but at a different axon location. Single trace. (D) Three superimposed traces from motor giant axon, same location as C. Bathing medium, 127 mmol l^{-1} Mg^{2+} sea water (A,B), 150 mmol l^{-1} Mg^{2+} sea water (C,D).

24 Ωcm found for the subumbrella epithelium of the siphonophore *Chelophyes* can be attributed to a low resistance 'shunt' to the underlying endodermal sheet (Chain, Bone & Anderson, 1981).

Innervation of the myoepithelium

Aglantha exhibits two major patterns of behaviour: fast 'escape' swimming when the entire subumbrella myoepithelial sheet contracts and 'slow' swimming when contraction is more localized. For fast swimming, nerves in the margin of the bell ensure that impulses are initiated nearly simultaneously in all eight motor giant axons (Roberts & Mackie, 1980). Evidence of dye-coupling (Weber *et al.* 1982) is consistent with there being electrical coupling between motor giant axons and lateral neurones and on an occasion in which a lateral motor neurone was successfully penetrated it was observed to spike following stimulation of the motor giant axon (R. W. Meech, unpublished observation). Chemical synapses along each motor giant axon (Singla, 1978) provide a pathway for excitation to spread directly to the myoepithelium (Fig. 9), but excitation also spreads by way of the lateral motor neurones which also make synaptic contact with epithelial cells in a field which spreads at least half-way across the octant. So in fast swimming the motor giant axons do two things: they directly excite the myoepithelium at chemical synapses; they electrically excite lateral motor neurones whose branches make further chemical synapses over the whole surface of the myoepithelium and ensure widespread contraction. Conduction of this kind cannot be accounted for by a regenerative action potential in the epithelium because there is no event in the muscle which behaves like a simple regenerative spike of the kind described in other hydromedusae (Mackie & Passano, 1968; Spencer, 1978).

In all hydromedusae studied to date (reviewed by Satterlie & Spencer, 1983) the nerves that generate the swimming pattern are located in the margin, where they rapidly conduct impulses around the bell, and excite the muscle sheet virtually simultaneously on all sides through synapses located in all quadrants. Conduction within the muscle sheet itself is generally purely myoid. In *Polyorchis*, an exceptionally large medusa, excitatory nerves extend from the margin up the four radii, an arrangement which presumably reduces conduction time in the radial direction. 'Pure' myoid conduction in *Polyorchis* is very slow in the radial direction – approximately $5\,\mathrm{cm\,s^{-1}}$ (Spencer, 1978). It is surprising to find that *Aglantha*, a relatively small species, lacks a propagating myoid action potential but relies on a system of motor neurones to spread excitation across the muscle sheet. One reason for this arrangement certainly lies in the need for exceptionally rapid and synchronous excitation of the whole muscle sheet during escape locomotion, an activity unique to this species. Another reason for the elaborate innervation may be found in the existence of two types of swimming in *Aglantha*. In addition to the short latency, powerful contractions of the escape response, the animal performs 'slow swimming' – low amplitude contractions which are not uniform but which spread throughout the muscle field (Mackie, 1980). It is likely that two such different responses could not be achieved if contractions spread solely by myoid conduction. This provides an illustration of the general principle that, while epithelial conduction is appropriate for

the spread of simple, generalized responses, nerves become necessary where graded or local effector action is called for (Mackie, 1970).

Recent evidence from the large leptomedusan *Aequorea* (R. A. Satterlie, personal communication) suggests that, here too, myoid conduction has been abandoned in favour of a system which combines multiple nerve inputs over the muscle sheet with local, decremental spread within the epithelium from these dispersed synaptic sites. The advantage in this case seems to be that the amplitude of contractions can be reduced locally by inhibitory input to the swimming motor neurones, so making asymmetrical contractions possible.

The authors wish to express their thanks to the Director and staff of the Friday Harbor Laboratories, University of Washington for their hospitality during the course of this work, and to Dr Nancy Lane, Dr Peter McNaughton and Dr Roger Moreton for their help and suggestions. We also thank Dr Andrew Spencer for his comments on the manuscript. The work was supported by grants from the Natural Sciences and Engineering Research Council of Canada (Grant No. A1427) to GOM, from the U.S. National Institute of Health (Grant No. EY 02290) to RWM and from the Royal Society to RWM and AR. R. W. Meech is a Wellcome Trust Senior Lecturer in Physiology.

REFERENCES

ABRAMOWITZ, M. & STEGUN, I. A. (1965). *Handbook of Mathematical Functions*. National Bureau of Standards Applied Mathematics Series, **55**. Washington, D.C.: U.S. Government Printing Office.

BARR, L., DEWEY, M. M. & BERGER, W. (1965). Propagation of action potentials and the structure of the nexus in cardiac muscle. *J. gen. Physiol.* **48**, 797–823.

BLOEDEL, J. R., GAGE, P. W., LLINÁS, R. & QUASTEL, D. M. J. (1966). Transmitter release at the squid giant synapse in the presence of tetrodotoxin. *Nature, Lond.* **212**, 49–50.

CHAIN, B. M., BONE, Q. & ANDERSON, P. A. V. (1981). Electrophysiology of a myoid epithelium in *Chelophyes* (Coelenterata: Siphonophora). *J. comp. Physiol.* **143**, 329–338.

COLE, K. S. (1968). *Membranes, Ions and Impulses*. Berkeley, Los Angeles: University of California Press.

DETWILER, P. B. & HODGKIN, A. L. (1979). Electrical coupling between cones in turtle retina. *J. Physiol., Lond.* **291**, 75–100.

DONALDSON, S., MACKIE, G. O. & ROBERTS, A. (1980). Preliminary observations on escape swimming and giant neurons in *Aglantha digitale* (Hydromedusae: Trachylina). *Can. J. Zool.* **58**, 549–552.

EISENBERG, R. S. & JOHNSON, E. A. (1970). Three-dimensional electrical field problems in physiology. *Prog. Biophys. molec. Biol.* **20**, 1–65.

FATT, P. & KATZ, B. (1951). An analysis of the end-plate potential recorded with an intracellular electrode. *J. Physiol., Lond.* **115**, 320–370.

FRÖMTER, E. (1972). The route of passive ion movement through the epithelium of *Necturus* gallbladder. *J. Membrane Biol.* **8**, 259–301.

HERNANDEZ-NICAISE, M.-L., MACKIE, G. O. & MEECH, R. W. (1980). Giant smooth muscle cells of *Beroë*. Ultrastructure, innervation, and electrical properties. *J. gen. Physiol.* **75**, 79–105.

JACK, J. J. B., NOBLE, D. & TSIEN, R. W. (1975). *Electric Current Flow in Excitable Cells*. Oxford: Clarendon Press. pp. 83–97.

JOSEPHSON, R. K. & SCHWAB, W. E. (1979). Electrical properties of an excitable epithelium. *J. gen. Physiol.* **74**, 213–236.

KATZ, B. & MILEDI, R. (1965*a*). The measurement of synaptic delay and the time course of acetylcholine release at the neuromuscular junction. *Proc. R. Soc. B* **161**, 483–495.

KATZ, B. & MILEDI, R. (1965*b*). The effect of temperature on the synaptic delay at the neuromuscular junction. *J. Physiol., Lond.* **181**, 656–670.

KATZ, B. & MILEDI, R. (1965*c*). The effect of calcium on acetylcholine release from motor nerve terminals. *Proc. R. Soc. B* **161**, 496–503.

LESTER, H. A. (1970). Transmitter release by presynaptic impulses in the squid stellate ganglion. *Nature, Lond.* **227**, 493–496.

MACKIE, G. O. (1970). Neuroid conduction and the evolution of conducting tissues. *Q. Rev. Biol.* **45**, 319–332.

MACKIE, G. O. (1980). Slow swimming and cyclical "fishing" behavior in *Aglantha digitale* (Hydromedusae: Trachylina). *Can. J. Fish. aquat. Sci.* **37**, 1550–1556.

MACKIE, G. O. & MEECH, R. W. (1985). Separate sodium and calcium spikes in the same axon. *Nature, London* **313**, 791–793.

MACKIE, G. O. & PASSANO, L. M. (1968). Epithelial conduction in Hydromedusae. *J. gen. Physiol.* **52**, 600–621.

PAYTON, B. W., BENNETT, M. V. L. & PAPPAS, G. D. (1969). Permeability and structure of junctional membranes at an electrotonic synapse. *Science, N.Y.* **166**, 1641–1643.

REVEL, J. P. & KARNOVSKY, M. J. (1967). Hexagonal array of subunits in intercellular junctions of the mouse heart and liver. *J. Cell Biol.* **33**, C7–C12.

ROBERTS, A. & MACKIE, G. O. (1980). The giant axon escape system of a hydrozoan medusa, *Aglantha digitale*. *J. exp. Biol.* **84**, 303–318.

SATTERLIE, R. A. & SPENCER, A. N. (1983). Neuronal control of locomotion in hydrozoan medusae. *J. comp. Physiol.* A**150**, 195–206.

SHIBA, H. (1971). Heaviside's "Bessel cable" as an electric model for flat simple epithelial cells with low resistive junctional membranes. *J. theor. Biol.* **30**, 59–68.

SINGLA, C. L. (1978). Locomotion and neuromuscular system of *Aglantha digitale*. *Cell Tissue Res.* **188**, 317–327.

SPENCER, A. N. (1978). Neurobiology of *Polyorchis*. I. Function of effector systems. *J. Neurobiol.* **9**, 143–157.

SPENCER, A. N. (1982). The physiology of a coelenterate neuromuscular synapse. *J. comp. Physiol.* **148**, 353–363.

TAKEUCHI, A. & TAKEUCHI, N. (1962). Electrical changes in the pre- and postsynaptic axons of the giant synapse of *Loligo*. *J. gen. Physiol.* **45**, 1181–1193.

WEBER, C., SINGLA, C. L. & KERFOOT, P. A. H. (1982). Microanatomy of subumbrellar motor innervation in *Aglantha digitale* (Hydromedusae: Trachylina). *Cell Tissue Res.* **223**, 305–312.

WOODBURY, J. W. (1962). Cellular electrophysiology of the heart. In *Handbook of Physiology*, Vol. I, Section 2. Washington: American Physiological Society. pp. 237–287.

WOODBURY, J. W. & CRILL, W. E. (1961). On the problem of impulse conduction in the atrium. In *Nervous Inhibition*, (ed. E. Florey), pp. 124–135. Oxford: Pergamon Press.